

Reassessing the dependence of cloud condensation nucleus concentration on formation rate

Andrew S. Ackerman*, Owen B. Toon†
& Peter V. Hobbs*

* Department of Atmospheric Sciences, University of Washington, Seattle, Washington 98195, USA

† NASA Ames Research Center, Moffett Field, California 94035, USA

MARINE stratocumulus clouds play an important role in the Earth's radiation budget. The albedo of these clouds depends on the cloud droplet size distribution, and therefore, in part, on the number density of cloud condensation nuclei (CCN)¹. It has been postulated² that a positive feedback loop between increased CCN concentrations and decreased drizzle gives rise to a bistable system, in which there are two equilibrium CCN concentration regimes. According to this model, CCN concentration is only weakly dependent on the CCN production rate within the stable regimes, but very strongly dependent on this rate in the transition region between the regimes. If correct, this strong dependence implies that a small increase in the production of CCN over the oceans could drastically increase the planetary albedo. Using a more sophisticated model³ than that used previously, we find no evidence for bistability. However, we find that CCN concentrations are generally strongly dependent on their production rate, so that changes in the latter would influence the Earth's albedo. We also find that the timescale for reducing high CCN concentrations can be as long as several days, which implies that high CCN concentrations can persist in clouds advected to regions of lower CCN production rate.

Baker and Charlson² (hereafter referred to as BC) suggested that the marine cloud-topped boundary layer is bistable with respect to CCN concentrations. When the production rate of CCN is low, the coalescence of droplets (which produces drizzle) maintains low CCN concentrations. Baker and Charlson identify this stable state with a clean marine boundary layer, with equilibrium CCN concentrations of ~ 5 – 50 cm^{-3} . At higher CCN concentrations in the BC model, cloud droplets were smaller and droplet coalescence was not efficient enough to balance the CCN production rate. A balance was not achieved until CCN concentrations reached $\sim 800 \text{ cm}^{-3}$; above this concentration the coagulation of dry CCN balanced their production rate. Because the albedo of marine stratiform clouds is sensitive to cloud droplet concentrations, the bistability hypothesis of BC suggests that global climate could depend on the production rate of CCN over the oceans in a highly nonlinear fashion.

In view of the potential importance of the BC bistability hypothesis, we have re-evaluated the relationship between CCN concentration and production rate using a more sophisticated model³. Both our model and the BC model assume that CCN are produced at a constant rate by unspecified processes; in other respects, the two models are quite different.

In the BC model, all unactivated CCN are assumed to be the same size. When liquid water is present, all CCN are assumed to activate to form droplets. The droplet spectrum is separated into two size classes: cloud droplets and drizzle drops. The reduction of particle concentration by droplet coalescence is calculated using an empirical formula to describe the drizzle flux and a simplified relationship to describe the efficiency with which drizzle drops collect cloud droplets. The cloud-microphysics component of our model⁴ resolves the size distributions of both unactivated CCN and cloud droplets into 50 size classes, ranging in radius from 0.005 to $500 \mu\text{m}$. Also, it treats explicitly the physical processes of CCN activation, droplet condensational growth and evaporation, the aggregation of particles due to thermal coagulation and the coalescence of particles due to gravita-

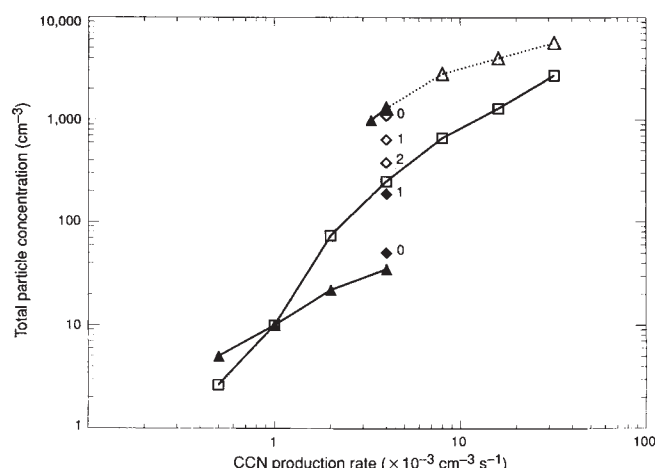


FIG. 1 Variation of equilibrium total particle concentration (N) averaged over the depth of the boundary layer, with CCN production rate (S_0). Squares connected by a solid line are results from the present model. Solid triangles connected by a solid line are results from the model of Baker and Charlson². Open triangles connected by a dotted line represent a balance between the CCN source and CCN sink by dry particle coagulation, using the formulation of Baker and Charlson. Also shown are the progressions toward equilibrium values of N from the present model simulations, starting with total concentrations of $1,100 \text{ cm}^{-3}$ (open diamonds) and 50 cm^{-3} (solid diamonds); the number alongside each point is the number of days elapsed after initialization. N reached the same equilibrium value after 2 and 3 days for initial values of 50 and $1,100 \text{ cm}^{-3}$, respectively.

tional collection. The single-layer model of BC considers the boundary layer to be well mixed and to have a prescribed depth. Our model resolves the boundary layer into ~ 40 layers, and treats turbulent transfer between layers⁵; boundary layer depth is determined by a dynamic balance between subsidence and turbulent mixing. The turbulent mixing in the BC model is driven by drizzle and a fixed net radiative flux loss from the boundary layer. Our model employs a sophisticated radiative transfer scheme⁶ that is coupled to the microphysical and thermodynamic fields. Baker and Charlson did not address time evolution issues because their steady-state model does not treat the dynamics between mixing, radiative transfer and cloud microphysics. Our model treats the evolution of the coupled system.

Although our model of the marine boundary layer is more detailed than the BC model, it has some shortcomings. Only one spatial dimension (the vertical) is represented. Therefore, horizontal heterogeneity and horizontal advection are ignored. Our treatment of vertical mixing assumes all turbulent transfer is down-gradient, which is not always the case. Only mean quantities are predicted by our model—variances are not treated. Despite these deficiencies, our model reproduces many of the observed characteristics of the cloud-topped marine boundary layer³. Model results compare well with measurements of stratiform cloud layers in the North Sea^{7,8}. In these comparisons, the model was able to reproduce measured variations (including drizzle rates) between clouds observed under different conditions.

To evaluate the sensitivity of CCN concentrations to CCN production, we ran our model with fixed boundary conditions to steady state (within the variation of diurnal oscillations). The only change between model runs was the CCN production rate (S_0), which we prescribed through the depth of the boundary layer using a log-normal aerosol distribution with a mean (by number) geometric radius of $0.1 \mu\text{m}$. For all our simulations, the model domain was initially cloudless and subsaturated with respect to water. The initial temperature lapse rate was adiabatic up to an inversion height of 750 m , where there were jumps in temperature ($+6 \text{ K}$) and water vapour mixing ratio (-2 g kg^{-1}).

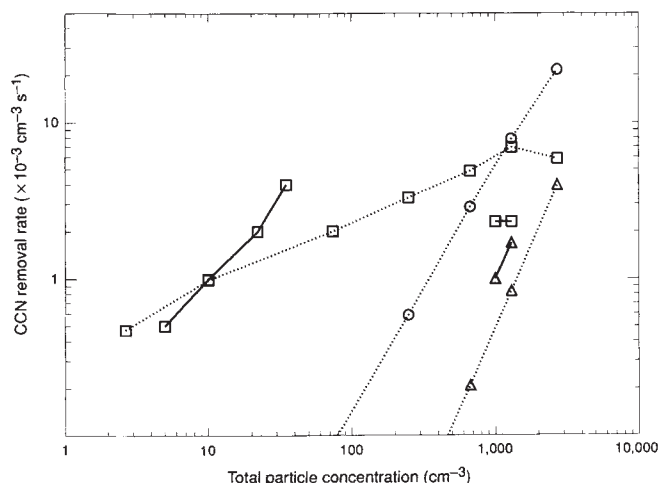


FIG. 2 Sink terms in the budgets for average total particle number concentrations (N) as a function of N . Dotted lines are from the present model, solid lines are from model of Baker and Charlson². In both cases, squares represent removal due to drizzle (by coalescence of droplets and deposition of drops on the ocean), and triangles represent particle removal due to coagulation between dry CCN. Collection of dry CCN particles by droplets in the present model is indicated by open circles.

At the lower boundary of the model, the sea surface temperature was fixed at 288 K. The downwelling infrared flux at the top of the model (1 km) was fixed at 270 W m^{-2} , and the wind speed in the top layer of the model was fixed at 8.5 m s^{-1} . The model simulations were started at midnight, with the sun rising four hours later and climbing to reach 35° from zenith, at noon. Over the long times required to reach steady-state conditions, the upward entrainment of the boundary layer was limited by a constant divergence rate of $5 \times 10^{-6} \text{ s}^{-1}$. Particles above the boundary layer were not advected downward by subsidence.

A comparison of our results with those of BC is shown in Fig. 1, where the total particle concentration (N) is the sum of the concentrations of unactivated CCN and cloud droplets averaged over the depth of the boundary layer. In this letter, N is referred to as the "CCN concentration". We have extended BC's results beyond the maximum source strength that they presented ($S_0 = 0.004 \text{ cm}^{-3} \text{ s}^{-1}$) by balancing the CCN source with the dry coagulation sink used in their model. Although the end points of the relationships from the two models are in agreement, the intermediate behaviour is very different. In contrast to the discontinuous jump in N at $S_0 \approx 0.004 \text{ cm}^{-3} \text{ s}^{-1}$ that the BC formulation gives, our model produces a smooth dependence of N on S_0 . The BC relationship between N and S_0 is nearly linear in both regimes. In our results the strongest dependency (nearly cubic) occurs in the region where N increases from 10 to 74 cm^{-3} in response to a doubling of S_0 from $0.001 \text{ cm}^{-3} \text{ s}^{-1}$. This peak in the N - S_0 dependence occurs in a regime where the effects of changes in CCN concentrations on radiatively driven turbulent mixing are greatest⁹.

The reasons for the differences between our results and those of BC are evident from the CCN removal rates shown in Fig. 2. In the BC model there are three sinks for CCN; dry particle coagulation, coalescence of cloud droplets with drizzle drops and deposition of drizzle drops to the ocean. We have combined the last two sinks and presented them as the removal rate of CCN by drizzle (only at the lowest CCN concentrations is droplet deposition significant). To understand our results, it is important to distinguish between the drizzle flux and the removal of droplets by coalescence, because they are not simply related. For instance, when N rises from 10 to $1,300 \text{ cm}^{-3}$ (and droplet concentrations rise from 7 to 500 cm^{-3}), the drizzle flux reaching the surface in our model decreases by a factor of 12 because the size of the drizzle drops decreases, but the removal of droplets

through coalescence increases by a factor of 7 because the number of droplets increases (Fig. 2).

At CCN concentrations below $\sim 50 \text{ cm}^{-3}$, droplet coalescence increases more rapidly with N in the BC model than in our model (Fig. 2). Therefore, at low CCN concentrations, N is less dependent on the CCN production rate in the BC model than it is in our model (Fig. 1). Droplet coalescence peaks at a droplet concentration of $\sim 50 \text{ cm}^{-3}$ in the BC model (Fig. 2). At higher particle concentrations, a balance with the CCN source can only be restored in the BC model when coagulation of CCN becomes significant. This gap in CCN concentrations, between where droplet coalescence is able to balance the CCN source and where dry coagulation is fast enough to maintain equilibrium CCN concentration, is called the "drizzle pause" by BC. The gap exists in the BC model because their total removal rate (the sum of drizzle removal and dry coagulation) initially decreases for droplet radii $< 10 \mu\text{m}$, which corresponds in their simulations to CCN concentrations $> 50 \text{ cm}^{-3}$. In our model, a decrease in droplet coalescence does not occur until much higher CCN concentrations are reached, where another removal process, the collection of CCN by droplets, is significant. There is neither a "drizzle pause" nor a discontinuity in equilibrium total particle concentrations in our model because the total removal rate never decreases as N increases.

The steady-state response of marine clouds to changing CCN production rates will not be realized unless the adjustment times are shorter than other relevant timescales (for example, the periods for which steady boundary conditions and steady CCN production rates prevail). We have evaluated the timescales required for CCN concentrations in the boundary layer to reach their equilibrium concentrations by performing model simulations in which N was initialized above and below its equilibrium value, and then following progress towards equilibrium. For both simulations, a source strength of $0.004 \text{ cm}^{-3} \text{ s}^{-1}$ was used, which produces an equilibrium N of 250 cm^{-3} (Fig. 1). To approach equilibrium from above, N was initialized at $1,100 \text{ cm}^{-3}$; equilibrium from below was approached by initializing N at 50 cm^{-3} . The progress of these simulations toward equilibrium is depicted in Fig. 3, where it is seen to take three days to reach equilibrium from an initial value of $1,100 \text{ cm}^{-3}$, while two days are required for the simulation initialized at 50 cm^{-3} . These are long periods of time relative to the time available for a cloud-topped marine boundary layer to evolve under conditions of roughly constant CCN production and steady boundary

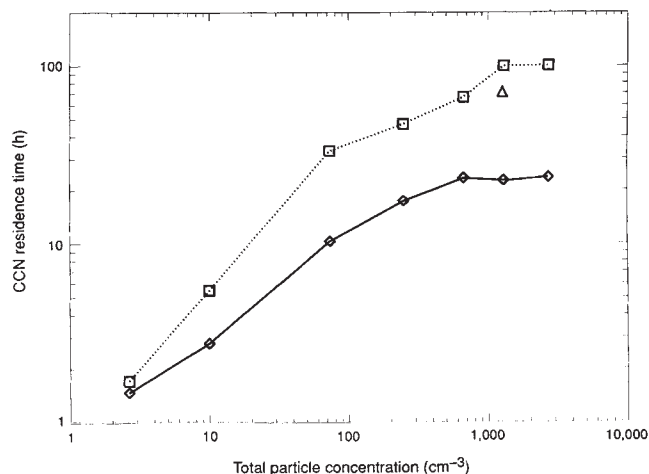


FIG. 3 Variations of CCN residence times (τ) with total particle number concentrations (N). Squares connected by the dotted line show residence time with respect to CCN mass concentration (τ_M). Diamonds connected by the solid line show residence time with respect to CCN number concentration (τ_N). Triangle is τ_M when the minimum deposition velocity is set to 0.1 cm s^{-1} .

conditions. For this reason, equilibrium CCN concentrations may often not be realized in nature. For example, marine boundary layer clouds that form in air with high CCN concentrations should retain high droplet concentrations for several days, provided that the microphysics of the cloud is determined by the CCN concentration rather than changing boundary conditions.

Residence times are another useful measure of CCN lifetimes. The residence time (τ) is equal to the equilibrium concentration of a quantity divided by its production rate. Using our results, the residence times for CCN number concentration (τ_N) and mass concentration (τ_M) are shown in Fig. 3. The three-day relaxation of N from an initial value of $1,100 \text{ cm}^{-3}$ to its equilibrium value of 250 cm^{-3} (Fig. 1) is consistent with an e-folding time of one day, which is close to the values shown in Fig. 3.

Because many processes that reduce CCN number concentrations do not affect CCN mass concentrations, τ_M always exceeds τ_N . As these two residence times can differ so much (Fig. 3), it is important to distinguish between them when estimating the effects of aerosols on cloud properties.

At low CCN concentrations, the deposition of drizzle on the ocean is the dominant sink for CCN mass, whereas the coalescence of cloud droplets is the dominant sink for CCN numbers. At high CCN concentrations, as the removal of CCN mass by drizzle reaching the ocean gradually becomes insignificant, τ_M is controlled by the dry deposition of CCN to the ocean. For CCN deposition velocities, we use the formulation of Giorgi¹⁰, in which the deposition velocity is a minimum ($\sim 0.01 \text{ cm s}^{-1}$) for particles of radius $\sim 0.1 \mu\text{m}$. Because CCN deposition veloci-

ties are uncertain, we ran an additional simulation in which the minimum value of the deposition velocity was 0.1 cm s^{-1} . This reduced our calculated value of τ_M by $\sim 25\%$, as shown in Fig. 3, but had negligible effect on τ_N .

Although we find no evidence of a bistability in the steady-state relation between CCN concentrations (N) and source strength (S_0), we agree with BC that N is strongly dependent on S_0 . Accordingly, there is a significant potential for changes in CCN production rates to change cloud droplet size distributions, cloud albedo, and therefore, climate. We find, however, it can take several days for N to reach equilibrium values. Therefore, clouds should be more sensitive to the highest CCN concentrations to which they are exposed than to the CCN production rates in regions to which they may be advected. \square

Received 9 November; accepted 9 December 1993.

1. Twomey, S., Piepgrass, A. M. & Wolfe, T. L. *Tellus* **36B**, 356–366 (1984).
2. Baker, M. B. & Charlson, R. J. *Nature* **345**, 142–145 (1990).
3. Ackerman, A. S., Toon, O. B. & Hobbs, P. V. *J. Atmos. Sci.* (Submitted).
4. Toon, O. B., Turco, R. P., Westphal, D., Malone, R. & Liu, M. S. *J. Atmos. Sci.* **45**, 2123–2143 (1988).
5. Duynkerke, P. G. & Driedonks, A. G. M. *J. Atmos. Sci.* **44**, 43–64 (1987).
6. Toon, O. B., McKay, C. P., Ackerman, T. P. & Santhanam, K. *J. Geophys. Res.* **94**, 16287–16301 (1989).
7. Nicholls, S. Q. *Jl. met. Soc.* **110**, 783–820 (1984).
8. Nicholls, S. & Leighton J. Q. *Jl. met. Soc.* **112**, 431–460 (1986).
9. Ackerman, A. S., Toon, O. B. & Hobbs, P. V. *Science* **262**, 226–229 (1993).
10. Giorgi, F. *J. Geophys. Res.* **91**, 9794–9806 (1986).

ACKNOWLEDGMENTS. This work was supported by NASA, the US DOE, the US ONR and the US NSF. We thank M. Baker and R. Charlson for discussions.

Rapid interglacial climate fluctuations driven by North Atlantic ocean circulation

Andrew J. Weaver & Tertita M. C. Hughes

School of Earth and Ocean Sciences, University of Victoria,
PO Box 1700, Victoria, British Columbia V8W 2Y2, Canada

RECENT data from the GRIP ice core^{1–3} in Greenland suggest that the climate of the last (Eemian) interglacial period was much less stable than that of the present interglacial. Rapid transitions between warm and cold periods were found to occur on timescales of just a few decades. The North Atlantic climate during the Eemian period was also shown to be characterized by three states, respectively warmer than, similar to and colder than today^{1,2}. Recent data from the nearby GISP2 ice core have revealed some discrepancies with these findings, which remain to be resolved^{4,5}. Here we present simulations using an idealized global ocean model, which suggest that the North Atlantic ocean has three distinct circulation modes, each of which corresponds to a distinct climate state. We find that adding a simple random component to the mean freshwater flux (which forces circulation) can induce rapid transitions between these three modes. We suggest that increased variability in the hydrological cycle associated with the warmer Eemian climate could have caused transition between these distinct modes in the North Atlantic circulation, which may in turn account for the apparent rapid variability of the Eemian climate.

One of the most important indicators of past climates and their variability is the record from the Greenland ice cores. Early analyses of these ice cores have shown that the climate of the North Atlantic during the last glaciation was marked by abrupt swings between relatively warm and relatively cold regimes^{6–8}. These climate shifts were observed to occur very rapidly (over several decades) and quite frequently (every several thousand

years or so). Similar oscillations have been found during the transition between the glacial and interglacial climates, the most recent of which was the Younger Dryas event which ended $\sim 10,000$ yr ago^{9–11}. Although it has long been known that the climate of our present Holocene period has been marked by much weaker natural climate variability on both the century¹² and decadal¹³ timescales, we have not observed any rapid and dramatic climate shifts.

The Greenland Ice-core Project (GRIP) 3028.8-m ice core from Summit, Greenland^{1,2} provides high-resolution climatic information through the Eemian and into the penultimate glaciation. The Greenland Ice Sheet Project 2 (GISP2) recently reported results from a 3,053.4 m core drilled 28 km to the west of the GRIP core^{4,5}. Although the two cores correlated extremely well over the top 90% of the record, the correlation in the rest

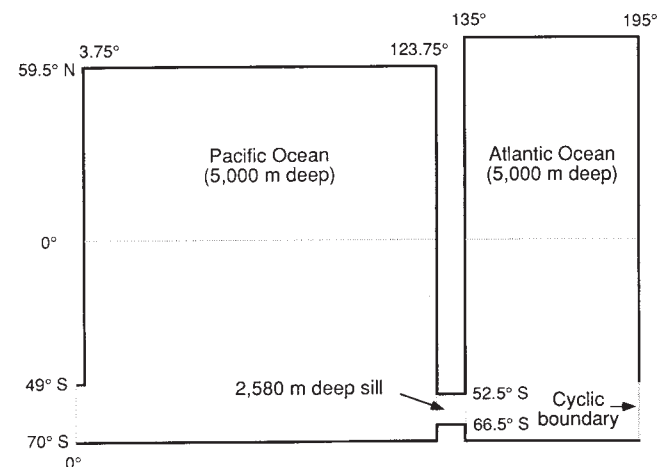


FIG. 1 The geometry (plan view) of the idealized two-basin model used in this study. All longitudes are measured relative to the western boundary of the model domain.